

PRELIMINARY RESULTS FROM THE USNO CESIUM FOUNTAIN

Thomas B. Swanson, U. S. Naval Observatory, Washington, D. C.
Eric A. Burt, U. S. Naval Observatory, Washington, D. C.
Christopher R. Ekstrom, U. S. Naval Observatory, Washington, D. C.

Abstract

We are pursuing a program that will integrate atomic fountain-based clocks into the U. S. Naval Observatory (USNO) Master Clock. We will present data from our cesium atomic fountain, including initial measurements of our device relative to an active hydrogen maser on both the clock transition and a magnetic field sensitive transition. As this maser is part of the USNO timing ensemble, we can easily relate the frequency and frequency stability of the fountain to any of our clocks or internal timescales. We will also present several possible continuous operation strategies for the incorporation of this new class of clock into the local clock ensemble.

Introduction

The last decade has seen advances in laser cooling and trapping that have allowed the practical construction of atomic fountain frequency standards. These devices are now producing results at several national standards institutions [1].

We have undertaken a program to integrate atomic fountain clocks into the timing ensemble at the USNO. The mission of the Observatory does not require that any of our standards be accurate realizations of the second, only that they be stable and run continuously. In support of that mission the observatory maintains an ensemble of atomic clocks that consists of approximately 50 commercial cesium-beam standards and 12 hydrogen masers. These standards are used to compute and produce several time scales, most importantly UTC(USNO). Our goal is to have several atomic fountain standards running with a short-term stability of $1-2 \times 10^{-13}$ and a statistical floor of $1-3 \times 10^{-16}$ to improve the medium- and long-term stability of the ensemble.

Because our goal is precision rather than accuracy, we are primarily interested in minimizing fluctuations in systematic contributions. Also, future devices will use rubidium in order to take advantage of the smaller cold-collision shift [2].

Experimental Layout

The physical layout of our fountain is shown in Figure 1. In addition to the small optical table that houses the vacuum chamber, there is a larger table that houses all of the lasers, with optical fiber coupling of all light onto the table with the vacuum chamber. All background pressures in the vacuum chamber are below 4×10^{-8} Pa.

Lasers

We collect atoms in either a magneto-optic trap (MOT) or molasses and then cool and launch them in an optical lattice with a (1,1,1) geometry. The laser light for the upward and downward directed laser beams originates with a low-power diode laser which is frequency stabilized and injection locks a second diode laser. The 100 mW output from this second laser separately injection seeds two tapered amplifiers with independent frequency control, and also provides the detection light. The collection and launching light from the tapered amplifiers and the detection light are transported to the vacuum chamber with optical fibers. All of these beams have power servos closed around the fiber path to reduce amplitude noise at the atoms. Collection and launching beams are expanded to 22 mm in diameter, with up to 30 mW of power per beam.

Launching

The atoms are launched in two phases. The first phase applies a violent acceleration for 1.4 milliseconds with an average detuning from resonance of 6 MHz. A second phase follows immediately with an average detuning of 40 MHz for 0.8 milliseconds, half the laser intensity, and a linear ramp of the intensity to zero at the end of the launch. We measure launch temperatures of 1.6 ± 0.2 μ K by monitoring the vertical width of the launched cloud when it passes the detection region both on the way up and on the way down, which allows us to remove the effects of initial cloud size.

State Selection

Immediately after launch, the atoms are pumped into the F=4 hyperfine levels with a vertical repumping beam

tuned to the $F=3$ to $F'=4$ transition. The atoms are state selected at the detection zone. They are exposed to a 3 millisecond long shaped pulse of 9.2 GHz microwaves from an axial loop antenna inside the vacuum chamber. This pulse transfers the $F=4, m_F=0$ atoms to the $F=3, m_F=0$ state. The remaining $F=4$ atoms are removed from the atomic sample by radiation pressure from a laser beam in the lower detection zone.

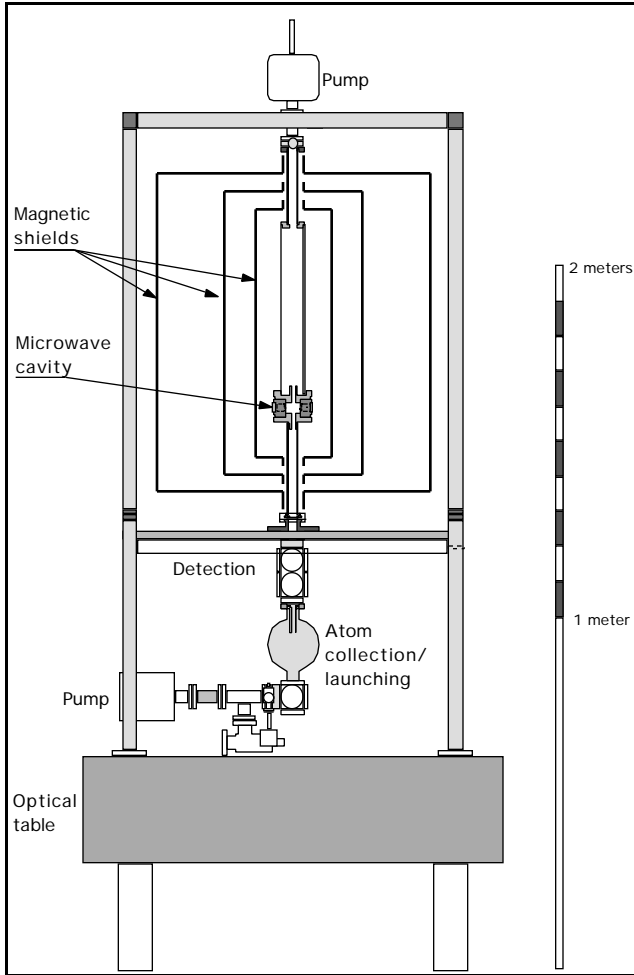


Figure 1: Cutaway mechanical view of the fountain.

Cavity, Shields and Drift Region

The microwave cavity and drift regions are temperature stabilized to 0.1 °C and enclosed in a set of three magnetic shields. The shields are made from 1.6 mm thick moly permalloy (MIL-N-14411B, “comp 1”) and have an axial shielding factor of 35,000, measured by observing the Rabi pedestal shift of atoms launched through the cavity with a known external field perturbation. Details of the construction of the shields have been provided previously [3]. An axial solenoid provides a 225 nT magnetic field for the cavity and free precession regions.

Detection

After making two transits of the microwave cavity the atoms return to the detection region. The upper detection zone monitors the $F=4$ population and the laser beam removes these atoms from the sample due to an imbalance in the radiation pressure. The radiation pressure is exerted by an imbalance in the retroreflected intensity of the laser and by detuning 2 MHz to the blue of resonance. The remaining $F=3$ atoms are then optically pumped into the $F=4$ state by a thin sheet of light tuned to the $F=3$ to $F'=4$ transition. The lower detection zone monitors the $F=3$ population by detecting these optically pumped atoms. The signals are collected, background levels are subtracted from each signal, and the $F=4$ signal is normalized by the sum of the $F=3$ and $F=4$ signals.

We run the fountain with a total cycle time between 1.1 and 1.9 seconds.

Results

Data were taken for experiments involving both the clock transition and a magnetic field sensitive transition. The local oscillator for these experiments is an active hydrogen maser from our clock ensemble. The microwave frequency chain is locked to a 100 MHz output of the maser. As the maser is separated from the fountain by a ~100 meter cable, we plan to move a maser into the same room as the atomic fountain in the near future.

Clock Transition

Figure 2 shows a microwave Ramsey resonance pattern on the $F=3, m_F=0$ to $F=4, m_F=0$ clock transition from our fountain.

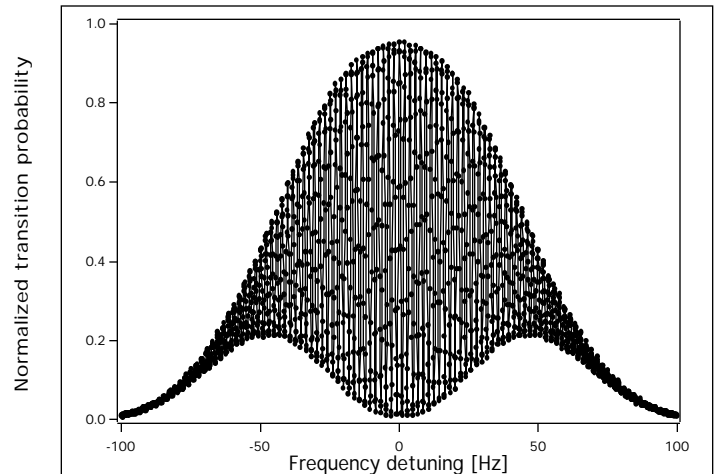


Figure 2: Normalized microwave resonance pattern on the $F=3, m_F=0$ to $F=4, m_F=0$ transition with no averaging. Cycle time is 1.9 seconds and the FWHM fringe width is 0.94 Hz. Lines connect data points only.

We have collected stability data by iteratively jumping between the half-height points on either side of the central fringe. The transition probability can be easily converted to a fractional frequency stability measurement of the local oscillator. Figure 3 shows the Allan deviation from a typical data set. The maser is more stable than the fountain on all time scales for this data set.

Because the maser is also monitored by our measurement systems, we can reference our frequency measurement of the maser to any other clock or average within our ensemble. This will also allow us to easily reference the long-term stability of our fountain to any other time scale, such as TAI or local realizations of UTC, which we monitor with our time transfer efforts.

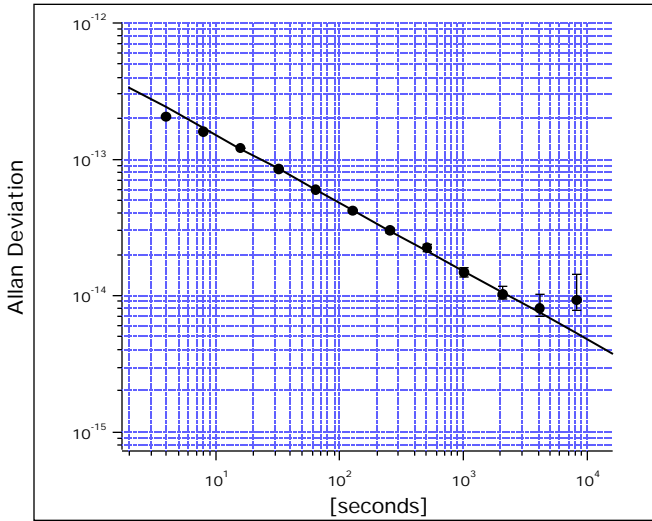


Figure 3: Stability of the fountain measured relative to an active hydrogen maser. The solid line is $4.75 \times 10^{-13} \tau^{-1/2}$ and is intended for reference only.

Magnetic Field Sensitive Transition

The fountain can also be run as a "flop-out" experiment, in which the atoms are not state selected prior to their transit of the microwave cavity, so all magnetic sublevels of the $F=4$ state are populated. The cavity is tuned to the $F=4, m_F = -1$ to $F=3, m_F = -1$ transition. The atoms then make the transition to the $F=3, m_F = -1$ state as the cavity is tuned through the resonance. Figure 4 shows the resulting Ramsey resonance pattern. A stability plot generated by iteratively jumping between the half-height points on either side of a central fringe for this transition show results that are consistent with a magnetic field fluctuation of less than 3 pT over $\sim 10^4$ seconds. This corresponds to a systematic fluctuation of $\sim 5 \times 10^{-18}$ on the field insensitive clock transition. Figure 5 shows the Allan deviation on the field sensitive transition.

During these experiments the MOT coils were turned off only for the launch and state selection phases, a duration of ~ 50 ms, in order to minimize the magnetic field fluctuations from shield relaxation.

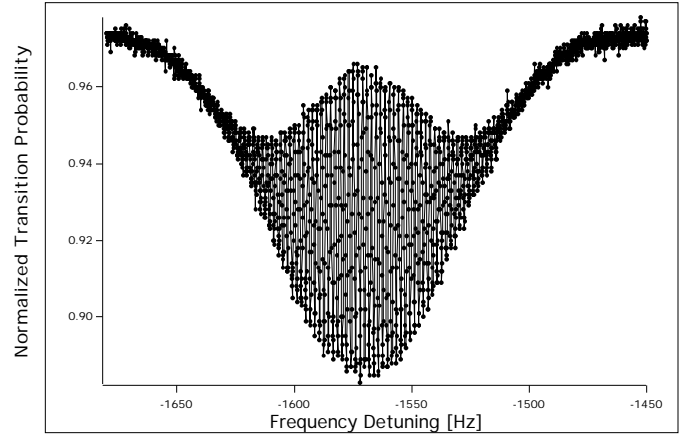


Figure 4. Normalized microwave resonance pattern on the $F=4, m_F = -1$ to $F=3, m_F = -1$ transition with no state selection. Lines connect data points only.

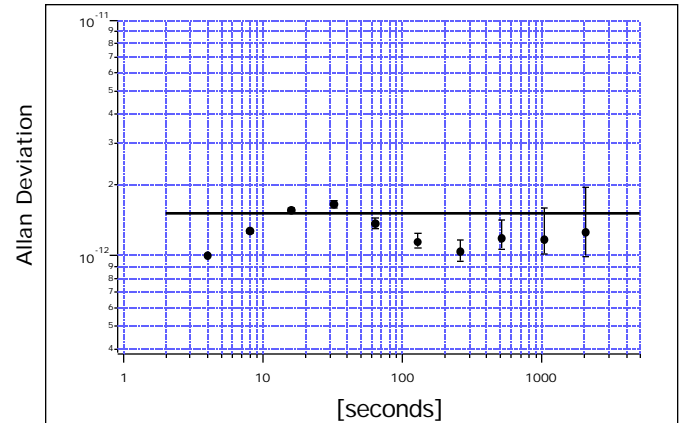


Figure 5. Stability of the fountain on the $F=4, m_F = -1$ to $F=3, m_F = -1$ transition at a relative detuning of -1571 Hz from resonance. The solid line is 1.5×10^{-12} and is intended for reference only.

Systematic Fluctuations

The magnetic field fluctuations measured on the $m_F = -1$ transition correspond to a field fluctuation in the lab of ~ 100 nT. External measurements show longer-term fluctuations limited to ~ 200 nT over a span of 10^5 - 10^6 seconds. At this level these fluctuations would contribute $\sim 1 \times 10^{-17}$ to our systematic floor, and the system could tolerate fluctuations several times larger, without the need for active cancellation of the external field. This would

still be an acceptably small contribution to our systematic floor.

Temperature fluctuations contribute via the blackbody shift and the temperature dependent cavity shift. Fluctuations of the cavity and drift region have been limited to 0.1 °C, which limit the combined systematic fluctuation below 5×10^{-17} .

Operational Possibilities

We are considering several possible ways of running our fountain as a continuous clock. The first is to directly steer a high quality quartz crystal. The short-term stability of our best crystal will require us to close our steering control loop in 2 to 4 seconds. The steering interval also sets the time scale over which the fountain can be allowed to not steer the local oscillator.

We are planning on using a different method of producing a steered, continuous output that employs an active hydrogen maser as a local oscillator. This would allow a steering time of roughly one hour for the class of masers at our disposal. The steered output would be monitored by our local measurement systems and would be introduced into our timescales in an identical manner to all other classes of clocks at the USNO. We anticipate that with our expected fountain performance and the measured drift rates of the masers in our ensemble, that the fountain should be steering out the maser drift starting at 1 to 20 days. The longer steering interval greatly reduces the stress on the operating duty cycle of the underlying atomic fountain at the addition of considerable cost for the maser and steering generator. In addition, the medium term stability of the unsteered maser is much better than that of an unsteered crystal.

It is our intention to build one more research device with rubidium atoms and to then produce up to five atomic fountains for operational use at the USNO and our alternate master clock facility in Colorado. We will use rubidium-based devices due to the dramatically smaller cold collision frequency shift [2].

Conclusions

In conclusion, we have observed reasonably high signal to noise microwave fringes in our atomic fountain with a preliminary stability of $4.8 \times 10^{-13} \tau^{-1/2}$ relative to an active hydrogen maser from our clock ensemble. We have identified potential noise sources that should allow us to reach our short-term stability goal of $1 - 2 \times 10^{-13} \tau^{-1/2}$.

We have measured the magnetic field fluctuation contribution to our systematic floor and estimated the contributions from temperature fluctuations. These appear to be consistent with meeting our systematic floor goal of $1 - 3 \times 10^{-16}$.

We have also outlined potential strategies for moving this class of device into continuous operation at the USNO.

References

- [1] A. Clairon, *et al.*, "Preliminary Accuracy Evaluation of a Cesium Fountain Frequency Standard" in *Proceedings of the Fifth Symposium on Frequency Standards and Metrology*, 1995, pp. 49-59; S. Bize, *et al.* "Interrogation Oscillator Noise Rejection in the Comparison of Atomic Fountains", pp. 9-11; S. R. Jefferts, *et al.*, "Preliminary Accuracy Evaluation of a Cesium fountain Primary Frequency Standard at NIST", pp. 12-15; S. Weyers, *et al.*, "First Results of PTB's Atomic Caesium Fountain", pp. 16-19; P. B. Whibberly, "Development of a Caesium Fountain Primary Frequency Standard at the NPL", pp. 24-26, all in *Proceedings of the conference EFTF and IEEE FCS*, 1999.
- [2] Y. Sortais, *et al.*, "An Evaluation of the Collisional Frequency Shift in a ^{87}Rb Cold Atom Fountain", pp. 34-38; C. Fertig, *et al.*, "Laser-Cooled Rb Fountain Clocks", pp. 39-42, both in *Proceedings of the conference EFTF and IEEE FCS*, 1999.
- [3] E. Burt, *et al.*, "Cesium Fountain Development at USNO", in *Proceedings of the conference EFTF and IEEE FCS*, 1999, pp. 20-23.